



Biodegradation of two persistent aromatic compounds by using oil shale

Miklós Molnár^a, András Hoffer^b, Judit Krisch^c, Rita Földényi^{a*}, Renáta Rauch^d, and Ottó Horváth^e 

^aSoós Ernő Water Technology Research and Development Center, University of Pannonia, Veszprém, Hungary; ^bMTA-PE Air Chemistry Research Group, University of Pannonia, Veszprém, Hungary; ^cInstitute of Food Engineering, University of Szeged, Szeged, Hungary; ^dResearch Institute of Bio-Nanotechnology and Chemical Engineering, University of Pannonia, Veszprém, Hungary; ^eDepartment of General and Inorganic Chemistry, Center for Natural Sciences, University of Pannonia, Veszprém, Hungary

ABSTRACT

Low-cost oil shale was investigated as a biodegradation promoter material, in order to exploit its potential for more widespread and efficient usage in the elimination of pollution. Degradation of two model pollutants, 4-nitrophenol and phenol, was examined in the presence of oil shale in a batch system. In order to investigate the role of the natural microflora of the oil shale in degradation, sodium azide was added to inhibit microbial growth. The effect of metal ions was also investigated. In the sodium azide-free solutions the model pollutants were completely degraded up to 2000 μmol/L concentration in a dose-dependent way, while the addition of sodium azide delayed greatly but did not stop the degradation. Manganese(II) ions increased the rate of the degradation of 4-nitrophenol, and given quantities of iron(II), manganese(II) or zinc(II) ions were also effective in degradation of phenol. Our results suggest that oil shale is not only an adsorbent but has an active role in the degradation of pollutants by its natural microflora. Utilizing these features of oil shale, it is a suitable candidate as an ameliorating agent, which can also be used in industrial size.

ARTICLE HISTORY

Received 27 May 2021
Accepted 30 August 2021

KEYWORDS

Biodegradation; decomposition; kinetics; 4-nitrophenol; organic pollutants

Introduction

The application of numerous persistent compounds by the chemical industry and pesticides by agricultural activities carries the danger of pollution of the environment because the appearance of these chemicals in nature can cause a long-lasting contamination. Furthermore, these pollutants can risk animal and human health by consuming foods exposed to these unhealthy compounds as well. That is why it is not surprising that the environmental protection and remediation has been a popular topic for a long time. Removal of the pollutants can be executed in different ways such as adsorption or degradation; biodegradation has also been utilized to remove these chemicals from the environment.^[1–8] In several studies, a given or a mixture of microorganism(s) was described to effectively degrade the target chemical. Natural materials or their extract which contain a mixture of microorganisms such as soil microflora could also eliminate the target compounds.^[6–8]

Sedimentary rocks from which oil can be extracted are commonly referred as oil shale. Oil shale is a lamellar sedimentary rock consisting of main residue of *Botryococcus braunii* microalgae, calcite, illite, and montmorillonite. It usually has a high organic material content, which is primarily kerogen. During the formation of oil shale in calm milieu lagoons or non-active volcanic craters filled with lakes, the residues of mainly propagated microalgae and

animals mixed with spores, pollens, and other floral residues, settled, anaerobically decayed, and aggregated as a rotting sludge. The water surface on these formation sides was covered by thick swamp vegetation, allowing only the super-fine alluvial grains to pass through. The calm, stagnant water was occasionally swollen by floods. At times, coarser particles also entered into the settling basin. The alteration of floods and the calm sedimentation periods created stratifications. The formation of oil shale took place over millions of years. There are numerous huge deposits of oil shale throughout the world, including Hungary. Because of its low price and versatility, the utilization of oil shale is multifarious: it is applied as a soil-ameliorating agent, starter fertilizer, adsorbent for bonding pollutants, clarifier, raw material for the production of fuel, skin-regenerative agent and medicine for curing skin disorders and articular diseases.^[9,10]

In this study, the degradation of two chemicals, 4-nitrophenol and phenol, were investigated as model pollutants in the presence of oil shale. Both compounds are frequently used in industry; thus, there are relevant risks of their emergence in nature. 4-nitrophenol has been utilized in the production of pharmaceutical drugs, dyes, explosive materials, agrochemical products, plasticizers, and wood preservatives. Furthermore, 4-nitrophenol can accumulate in nature by hydrolysis of organophosphorus insecticides, and nitrophenolic herbicides as well.^[5,11]

Phenol has been used in the production of a large group of chemicals such as the examples mentioned in 4-nitrophenol. Furthermore, there is a huge quantity of polycarbonates, phenolic resins, and other polymers. Nowadays, there is a high demand for phenol, with a total production capacity of more than 13 megatons in 2020. In addition, phenol can also be found in nature. It occurs in coal tar and in small quantity in pine trees as well.^[12,13] Both chemicals are considered as priority pollutants, according to the Environment Protection Agency (USA, EPA).

The present study investigates not only the transformation effect of the examined Hungarian oil shale on substrates but also the added supplementary metal salts.

Although the effect of heavy metals on soil microorganism is usually deteriorative, and the amount of microbial biomass decreases.^[14] There are some species, which can tolerate them^[14,15]; moreover, in some cases, the added metal ions enhance the activities of enzymes involved in substrate degradation.^[5,16] In addition, the activity of several fungi increases by metal contamination. In some cases, the fungal/bacterial ratio increases by the addition of a metal salt into the system; the higher amount of metal loaded, the higher ratio can be observed.^[17]

The main goal of this study was to explore how effectively the low-price Hungarian oil shale can biodegrade two model pollutants in the liquid phase, and whether this effect could be improved by the addition of metal salts or in another way. These results can be utilized in the consideration of the industrial application of the investigated oil shale in the future.

Materials and methods

Materials

Maar-type oil shale was collected in Pula, Hungary. The mining raw oil shale was air-dried and milled to a particle size of $\phi < 800 \mu\text{m}$. Acros Organics supplied the 4-nitrophenol, copper(II) chloride, and iron(III) chloride hexahydrate. Calcium chloride, anhydrous pyridine, N-1-naphthylethylenediamine dihydrochloride, and N,O-Bis(trimethylsilyl)trifluoroacetamide (BSTFA) with 1% trimethylchlorosilane (TMCS) were purchased from Lach-Ner s.r.o., Merck KGaA, Alfa Aesar, and Macherey-Nagel GmbH, respectively. Manganese(II) chloride tetrahydrate and hydrazine sulfate were received from Reanal Laborvegyszer Kft. HPLC grade methanol and zinc(II) chloride were obtained from Fisher Chemical Co. Sulfanilamide and copper(II) sulfate pentahydrate were collected from Molar Chemicals Kft. HPLC grade ethyl acetate, phenol, sodium azide, and iron(II) sulfate heptahydrate were acquired from VWR International Ltd. All chemicals were used without further purification.

Analytical methods

Characterization of the utilized oil shale

In our previous work, the identical Hungarian oil shale was utilized as a sorbent; thus, it was already characterized. The

details and methods of X-ray diffraction and Scanning Electron Microscope (SEM) measurements have been described in our previously reported article.^[18]

Determination of concentration of 4-nitrophenol and phenol

Concentrations of 4-nitrophenol or phenol were determined by a Merck Hitachi LaChrom HPLC system (Tokyo, Japan) equipped with a Waters Nova-Pak C18 column ($75 \times 3.9 \text{ mm}$, $4 \mu\text{m}$, 60 \AA) and programmable UV detector. The mobile phase was 30% or 15% methanol in Milli-Q water; the pH was adjusted to 4.3. The flow rate was 1 mL/min. A $10 \mu\text{L}$ sample was injected into the column by an autosampler, and the absorbance values of 4-nitrophenol or phenol were recorded at 317 or 270 nm. The retention time was around 3.6 or 3.5 minutes. The calibration curve was generated by measuring 4-nitrophenol or phenol standards in the concentration range from 5 to $500 \mu\text{mol/L}$ or from 50 to $1000 \mu\text{mol/L}$ ($R^2 > 0.99$), respectively. The concentration of the samples was calculated from the slope of the calibration curve. The limits of detection of 4-nitrophenol and phenol were 0.1 and $1 \mu\text{mol/L}$, respectively. The pH values were measured by a Radelkis combination pH electrode (Budapest, Hungary).

Qualitative analysis of degradation products of 4-nitrophenol and phenol by gas chromatography-mass spectrometry (GC-MS)

The extraction is performed on both the supernatant (the liquid phase which was contacted with the oil shale, and initially contained $500 \mu\text{mol/L}$ 4-nitrophenol or phenol and $0.01 \text{ mol/L CaCl}_2$) and the oil shale sludge separately. Approximately 6 g of sludge or 30 mL of supernatant was sampled periodically. These samples were acidified under pH 2 by the addition of hydrochloride acid, then 20 – 20 mL ethyl acetate was added to the sludge or supernatant, and agitated in a horizontal shaker for 60 minutes at a rate of 90 cycles per minute at room temperature. The ethyl acetate phase was drawn off, filtered through a hydrophilic PTFE membrane syringe filter ($0.45 \mu\text{m}$ pore size), and the solvent was completely evaporated under a nitrogen stream at room temperature. For silylation, $100 \mu\text{L}$ of pyridine and $100 \mu\text{L}$ of BSTFA-MTCS were added to the dried extract, and this solution was incubated at 80°C for 60 minutes.

The GC-MS measurements were carried out on an Agilent 6890 N gas chromatograph (China) equipped with an Agilent DB-5MS UI capillary column ($30 \text{ m} \times 0.25 \text{ mm} \times 0.25 \mu\text{m}$), coupled to an Agilent 5973 N mass spectrometer (USA). $1 \mu\text{L}$ of this derivatized sample was injected automatically into the GC-MS injector (temperature: 290°C , splitless mode). The column temperature was 60°C for 1 minute, then was increased to 320°C at a rate of 10°C/minute , and was held for 15 minutes. The total run time was 42 minutes. The measurements were conducted in scan mode (m/z : 14 – 500).

The samples extracted from the liquid (supernatant) and the solid (sludge) phases were measured separately. Blank

samples were also measured for both substrates (4-nitrophenol and phenol) by the above-described method, from the liquid and solid phases independently.

Determination of the concentration of sodium azide

The concentration of sodium azide in the supernatant was measured photometrically as a ferric azide complex.^[19] 1.8 mL of 50 mmol/L iron(III) chloride, which was prepared with 10 mmol/L hydrochloric acid, was mixed with 0.2 mL of the supernatant of the sample. This mixture was incubated for 5 minutes, and the absorbance values were recorded with a Varian Cary 50 UV-Vis spectrophotometer (Mulgrave, Victoria, Australia) at 458 nm, using a 0.5-cm-path-length quartz cuvette. Before quantification, a calibration curve was constructed by measuring sodium azide standard solutions of different concentrations and utilized to calculate the concentration of the samples.

Determination of the concentration of nitrite and nitrate ions

The concentration of nitrite ion was determined using the Griess-Ilosvay method by diazotization reaction. The concentration of nitrate ion was defined as nitrite, after the reduction of nitrate into nitrite ions. 0.5 mL of supernatant was measured into a test-tube and diluted with 4.5 mL 0.05 mol/L sodium hydroxide solution. A 250 μ L copper working solution (containing 0.1 g/L copper(II) sulfate pentahydrate and 0.2 mL/L concentrated sulfuric acid in water) and a 350 μ L 16.5 g/L hydrazine sulfate solution were added to the diluted sample and mixed thoroughly. It was incubated at 40 °C for 10 minutes, and then 1 mL color reagent (containing 10 g/L sulfanilamide, 1 g/L N-1-naphthylethylenediamine dihydrochloride, and 34 mL/L concentrated sulfuric acid in water) was added and mixed. After 5 minutes of incubation at room temperature, the absorbance values were recorded with a Varian Cary 50 UV-Vis spectrophotometer at 534 nm. Using a calibration curve, the concentration of the sum of nitrite and nitrate ions was calculated. The concentration of nitrite ions was measured by using almost the same procedure, except the hydrazine sulfate and copper working solution were replaced by deionized water.

Hot-water extractable carbon determination

Hot-water extractable carbon (HWC) extraction was carried out similarly to that described by Ghani et al.^[20] 3 g of oil shale powder was weighed into a 50 mL centrifuge tube, and 3 mL of deionized water was added to the powder. The oil shale was left to swell overnight, and 30 mL of deionized water was poured onto the swollen oil shale powder. This suspension was mixed in an end-over-end shaker at 30 rpm for 30 minutes at room temperature, then it was centrifuged at 3500 rpm for 20 minutes. The supernatant was separated from the oil shale powder, and the liquid phase was filtered through a membrane filter (0.45 μ m pore size). This portion is called water-soluble carbon (WSC). Another 30 mL of deionized water was poured onto the same oil shale sludge,

the powder was suspended by a vortex shaker, and the suspension was incubated at 80 °C for 16 hours. At the end of the incubation period, the tube was vortexed, centrifuged (3500 rpm for 20 minutes), and the supernatant was filtered through another membrane filter (0.45 μ m pore size). This fraction was named HWC. The total organic carbon (TOC) contents of both the HWC and the WSC fractions were determined by a Shimadzu TOC-L analyzer (Kyoto, Japan). The samples were in triplicate.

Analysis of the microbial community on oil shale

A detailed description of the analysis can be found in the work by Lázár et al.^[21] Briefly, bacterial DNA was extracted from approximately 200 mg of oil shale using the ZymoBIOMICS 96 MagBead DNA Kit. A Thermo Fisher Scientific Qubit 3.0 Fluorometer (Waltham, MA, USA) and the Qubit dsDNA HS Assay Kit were used to determine the concentration of genomic DNA. The V3–V4 region of the bacterial 16S rRNA gene was amplified. High Sensitivity D1000 ScreenTape on an Agilent 2200 TapeStation instrument (Waldbronn, Germany) was used to quantify and qualify the PCR product libraries. The generated raw sequencing reads were quality-filtered using Illumina MiSeq Control Software. The classification was executed by an Illumina 16S Metagenomics workflow based on the DADA2 formatted RefSeq RDP 16S v3 database.

Degradation experiments

25 g of oil shale powder was weighed into 720 mL sterilized (at 140 °C for 2 hours) stoppered glass flasks. 25 mL of deionized water or one of various metal salt solutions, 5, 10, 20 or 40 mg/L sodium azide, 15 μ mol/L or 154 mmol/L manganese(II) chloride, iron(II) sulfate, copper(II) chloride or zinc(II) chloride, was added to this oil shale powder in each experiment – notably, one solution contained only one metal salt. This oil shale was left to swell overnight at room temperature. Thereafter 250 – 250 mL of an initial concentration of 500 μ mol/L 4-nitrophenol or phenol solution, containing 0.01 mol/L CaCl₂ (pH = 7.6) was poured onto the swollen oil shale powder samples, and these suspensions were shaken for 24 hours on a horizontal shaker until adsorption equilibrium was obtained. From this point, the degradation process was monitored. The glass flasks were stored in a dark place at room temperature. A small amount of supernatant was taken periodically and centrifuged in Eppendorf tubes at 15000 rpm for 20 minutes, and then the actual concentration of 4-nitrophenol or phenol was measured by HPLC-UV. All samples were in triplicate.

Origin 6.1 scientific graphing and analysis software was used for visualization. The fitting procedure of the kinetic models to the degradation curves was executed by nonlinear optimization using the generalized reduced gradient method of Microsoft Excel Solver. Analysis of variance (ANOVA) calculation was performed on the GraphPad Prism 9.1.0 software.

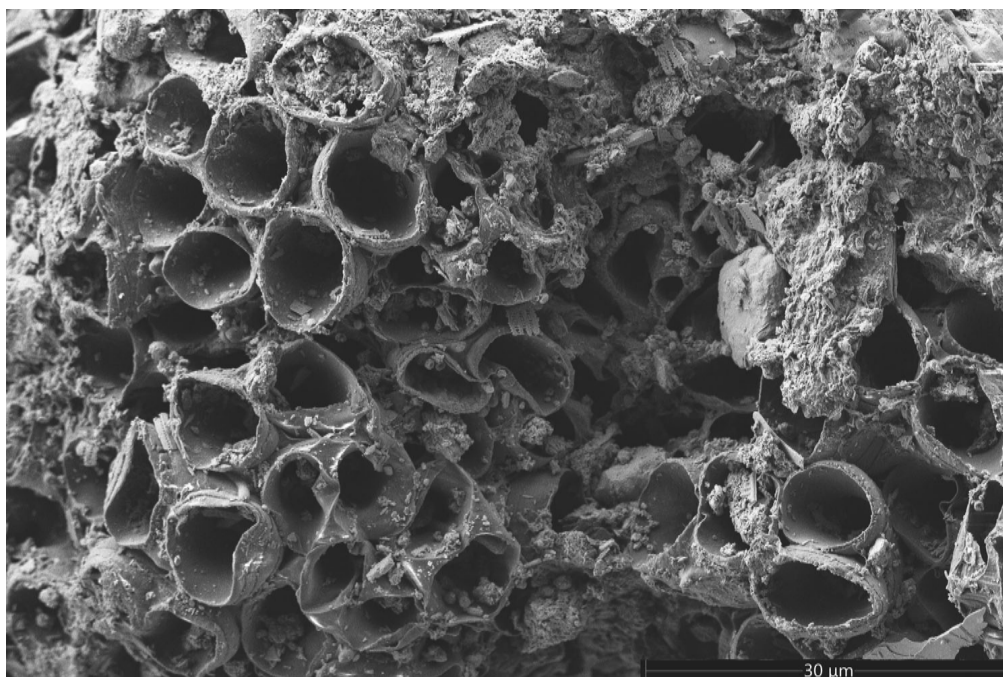


Figure 1. SEM image of Hungarian oil shale with diatoms fossils.

Results and discussion

Characterization of oil shale

The characterization results of X-ray diffraction measurement of the applied oil shale are the following: The main mineral fractions were smectite (28%), aragonite (17%) and calcite (12%). Smectite was responsible for the swelling capability of the oil shale. Other mineral fractions were mica (7%), mixed Fe–Mg-carbonates (7%), dolomite (7%), plagioclase (5%), quartz (4%), kaolinite and chlorite (3%), gypsum (2%). The remaining value (8%) can correspond to the amorphous phase. Further details of the used oil shale can be found in our previous article.^[18]

The hot-water extractable carbon (HWC) value of the used Hungarian oil shale was 1.44 mg C/g. Ghani et al.^[20] described that HWC is strongly and positively correlated with microbial biomass carbon, mineralizable nitrogen, extractable carbohydrate, and a slightly lower correlation can be obtained between HWC and microbial biomass nitrogen. Hence, the amount of organic nutrients available for microorganisms can be concluded from the HWC value, which ranged between 0.6 and 5.4 mg C/g in the investigated soils. The HWC of cropping soil (1.0 mg C/g) is the closest to the used oil shale sample (1.44 mg C/g), which means that the organic nutrient pool available for microorganisms in the oil shale is sufficient.

An SEM image of the used oil shale can be seen in Figure 1. The irregularly spherical to oval in shape cup-like formations connected to each other are the residues of fossilized alga (*Botryococcus braunii*) colonies. During the formation of oil shale, the inner cell content decayed, but the outer cell walls consist of insoluble and highly resistant biopolymers, Polymer Resistant *Botryococcus*, which survived the chemical degradation. This arrangement results in a pore-like structure of the oil shale.^[22,23]

Results of the degradation experiments

Results of degradation experiments of 4-nitrophenol and the effect of added sodium azide and metal ions

Figure 2 shows the rate of decay of 4-nitrophenol in different cases. The decay curve obtained with oil shale swollen with deionized water is the reference base because the oil shale was not modified by any additives. In this case, the complete decay of 4-nitrophenol took 12 days (initial concentration was 500 μmol/L). As it can be seen, the curve can be divided into two main sections: a slower initial (adaptation period), and a faster (second) decay stage of 4-nitrophenol. The change between the two sections was around the seventh day. We assume that in the first section the microbial community in the oil shale adapted to the new environment containing 4-nitrophenol. Thus, during this section, the decay of 4-nitrophenol was slower. Then in the second stage, the enzyme systems of the adapted microorganisms could degrade the substrate faster. Similar enzyme supported degradation of 4-nitrophenol described by Kowalczyk et al.^[24] was observed, where bacterial populations living in river water were utilized.

Sodium azide added to oil shale delayed the time of transformation of 4-nitrophenol. The extent of sodium azide intake influenced this retardation. When the oil shale was swollen with the lowest concentration of sodium azide solution (5 g/L, which is equal to 5 g NaN₃/1 kg oil shale), the total transformation was delayed to the smallest extent. The complete decay of 4-nitrophenol lasted 63 days. The following concentration value of sodium azide was 10 g/L. The time of delay was longer than in the former case. The complete transformation of 4-nitrophenol occurred in 108 days. As can be seen in Figure 2, in these two cases, a slower and a faster decay section have also appeared, but they are elongated, especially the adaptation period, compared to the reference base. The relatively sharp transition between the two

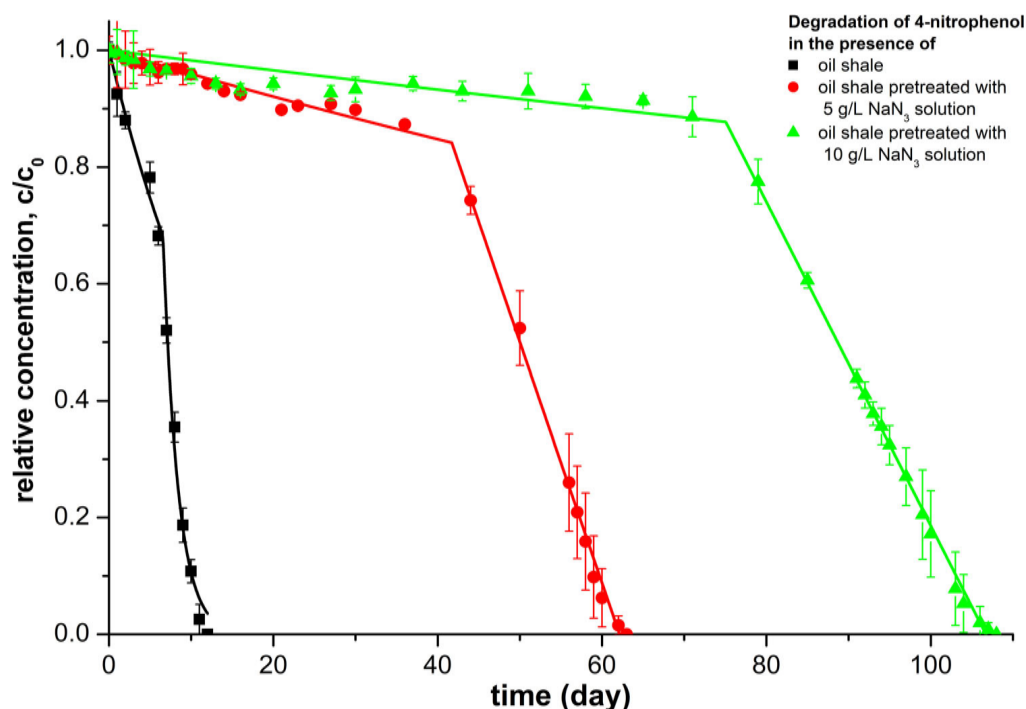


Figure 2. Degradation curves of 4-nitrophenol in the presence of oil shale without and with pretreatment with 5 and 10 g/L NaN_3 solutions.

sections occurred around the 42nd and 75th day, respectively. The next two concentration values of sodium azide were 20 and 40 g/L. In these cases, the perfect transformation of 4-nitrophenol could not be obtained within one year (> 365 days). These results confirmed that the transformation of 4-nitrophenol was of biological origin because the microorganisms' activity in the oil shale was inhibited by sodium azide. The extent of the retardation depended on the concentration of sodium azide, but the change in the amount of sodium azide in the supernatant was negligible over time (Fig. A1 in the Appendix). These findings confirm that, in the case of lower sodium azide concentrations, microorganisms can easily develop resistance to it. These results well agree with those found in the literature. An increased concentration of sodium azide creates greater inhibitory effect, even if the bacteria have previously formed sodium azide-resistance.^[25,26]

The effects of several metal salts, such as manganese(II) chloride, iron(II) sulfate, copper(II) chloride, and zinc(II) chloride, added in dissolved form to oil shale as a swelling solution, were also tested on the time of degradation of 4-nitrophenol. Manganese(II) chloride was the only one that provided a concentration-dependent faster decay of 4-nitrophenol as can be seen in Figure 3. Regarding the degradation time, the additions of the other metal salts were disadvantageous irrespective of their quantities. When manganese(II) chloride was used at a 154 mmol/L concentration, the time required for the complete transformation of 4-nitrophenol was decreased from 12 to 9 days. Its decay curve was similar to that of the reference base (degradation in the presence of oil shale swollen with deionized water). The change between the slower and the faster decay sections was around the sixth day. In the case of the lower concentration of manganese(II) chloride (15 $\mu\text{mol/L}$), the decay curve slightly differs from that of the higher concentration.

The complete decay of 4-nitrophenol occurred in 10 days. Interestingly, the faster decay section began later than that of the reference base on, at around the eighth day, but the degradation rate of 4-nitrophenol was significantly faster in this second phase. These results show that manganese(II) ions could enhance the degradation by increasing the enzyme activity of some microorganisms. Presumably, metalloenzymes produced by the microbial community in the oil shale could catalyze the transformation of 4-nitrophenol. Manganese(II) ions can activate them, whereas iron(II), copper(II), and zinc(II) ions can deactivate them. These modified enzyme activities could be related to their conformational changes, and manganese(II) ions could stabilize them or promote 4-nitrophenol binding to these enzymes by modifying their catalytic sites.^[16] Manganese(II) ions have also been reported as an enzyme activity enhancer related to 4-nitrophenol degradation by Zhang et al.^[5]

As a reference, degradation experiments without oil shale and metal salts were also performed, and there was not any remarkable decay of 4-nitrophenol by the end of the examination.

Results of degradation experiments of phenol and the effect of added sodium azide and metal ions

Similar to the previous subchapter, the reference base will be the decay curve with oil shale swollen with deionized water as can be seen in Figure 4. The complete transformation of phenol occurred in 9 days, three days earlier than in the case of 4-nitrophenol under the same experimental conditions. The shape of the decay curve of phenol was very similar to that of 4-nitrophenol, showing the two main sections. The transition between the two sections was around the fifth day. The reason would be the same as in the case of 4-nitrophenol, the microbial community whose enzyme

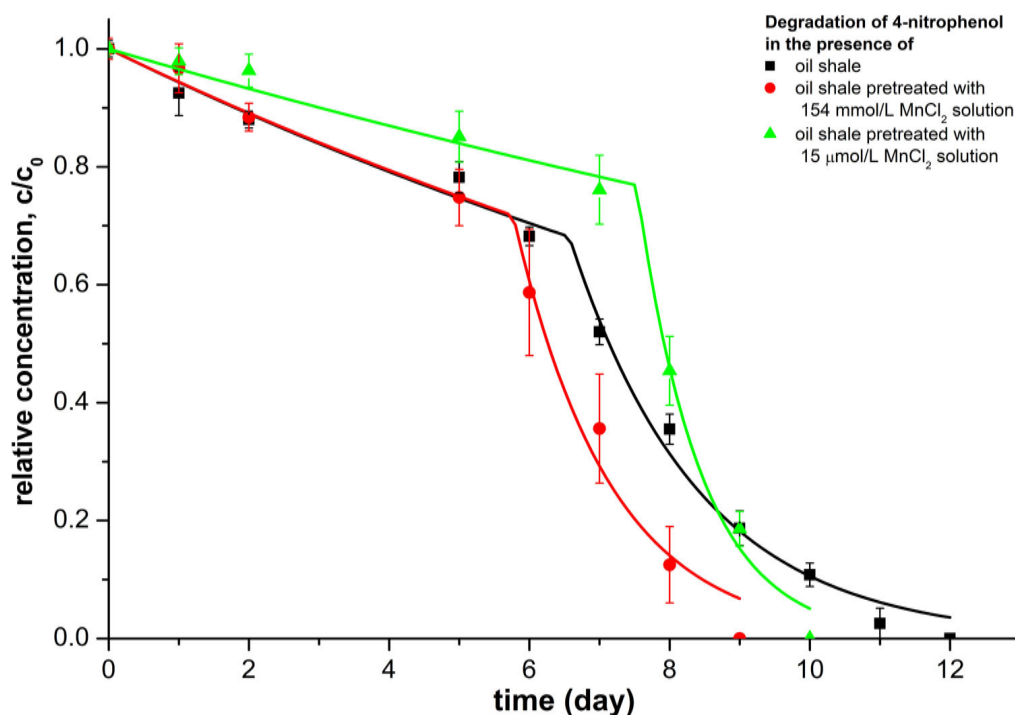


Figure 3. Degradation curves of 4-nitrophenol in the presence of oil shale pretreated with 154 mmol/L and 15 $\mu\text{mol/L}$ MnCl_2 solutions. For comparison, untreated oil shale is also illustrated.

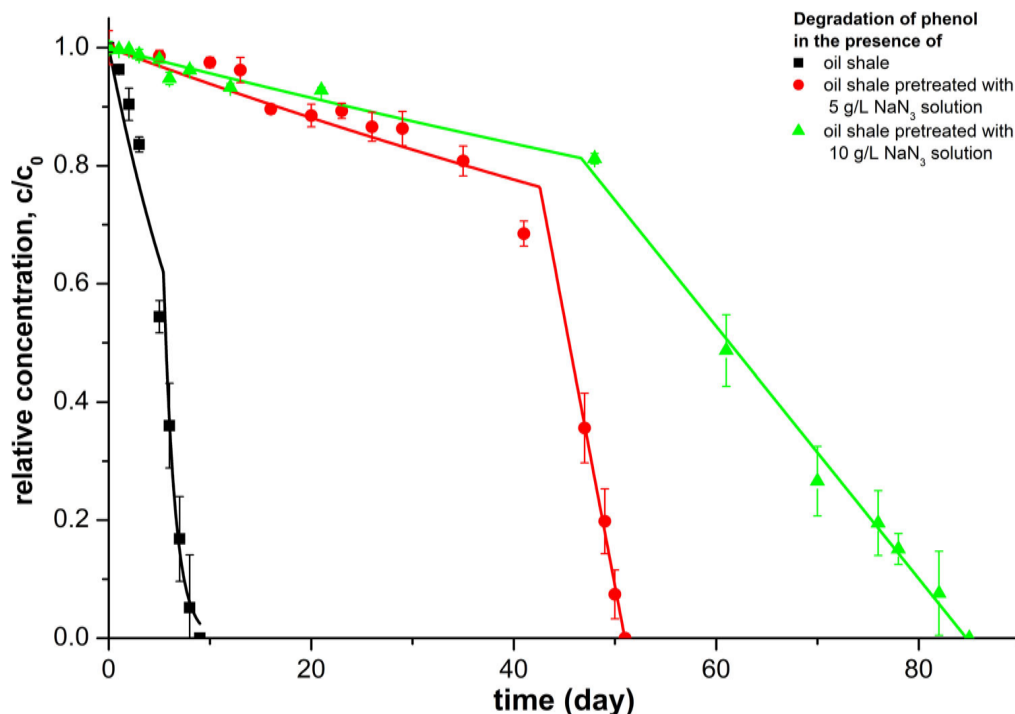


Figure 4. Degradation curves of phenol in the presence of oil shale without and with pretreatment with 5 and 10 g/L NaN_3 solutions.

systems were responsible for the transformation of phenol adapted to the new environment during the first stage. Meanwhile, a slower degradation of phenol occurred, followed by a faster decay of phenol by the adapted microorganisms. Similar degradation pattern was described by Kwon and Yeom,^[27] who investigated the degradation of phenol by *Pseudomonas fluorescens*.

The effect of sodium azide and its concentration dependence were also investigated. When the oil shale was swollen with the lowest concentration of sodium azide solution (5 g/L), the complete degradation of phenol occurred in

51 days. The shape of the decay curves is very similar to the previously described cases, and it can be divided into a slower and a faster phenol decay rate. The end of the elongated adaptation period was around the forty-third day. In the case of the 10 g/L of sodium azide swelling solution, the time of transformation of phenol was increased to 85 days. The transition between the two sections occurred around the forty-seventh day (Fig. 4). Similar to the case of 4-nitrophenol, when the oil shale was swollen by using 20 and 40 g/L sodium azide solution, degradation of phenol was negligible in the experiments.

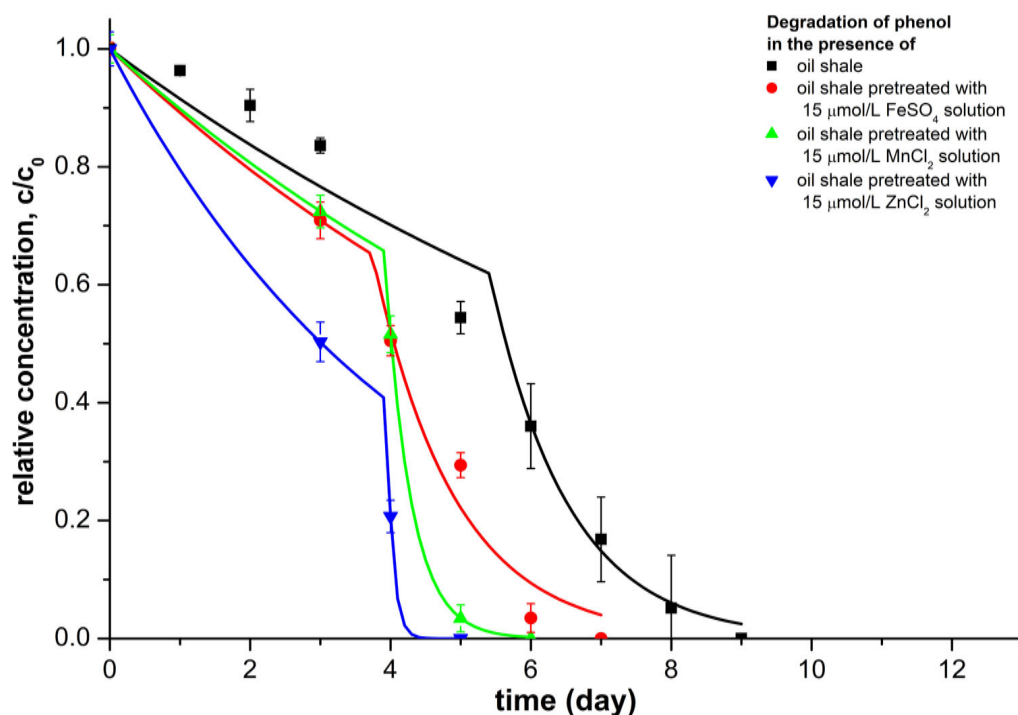


Figure 5. Degradation curves of phenol in the presence of oil shale pretreated with 15 $\mu\text{mol/L}$ FeSO_4 , MnCl_2 , and ZnCl_2 solutions. For comparison, untreated oil shale is also illustrated.

The addition of metal ions (manganese(II) chloride, iron(II) sulfate, copper(II) chloride, and zinc(II) chloride) to the oil shale had different effects than in the case of 4-nitrophenol. On the phenol substrate, the addition of a higher concentration of all the above-mentioned metal ions (154 mmol/L) decelerated the transformation of phenol. However, in the case of a smaller concentration of metal ions (15 $\mu\text{mol/L}$), iron(II), manganese(II), and zinc(II) ions could unequivocally decrease the time of degradation of phenol to 7, 6, and 5 days, respectively. In all cases, the transition between slower and faster decay sections occurred around the fourth day. These results can be seen in Figure 5.

As a reference, degradation experiments without oil shale and metal salts were also performed, and there was not any significant decay of phenol in the solution by the end of the examination.

Degradation of both substrates (4-nitrophenol and phenol) in the presence of individual metal ions without oil shale were also examined whether the added metal ions act as an inorganic catalyst during the degradation. There was not any notable concentration decrease during the experiments. These outcomes unambiguously indicated that alterations in the degradation time of the examined substrates by the addition of metal ions to the oil shale were of biological origin.^[5,28]

These above-described results would also suggest that the enzyme systems responsible for the transformation of phenol differ from that of 4-nitrophenol. According to literature data, the degradation pathways of phenol and 4-nitrophenol are comparable, but the initial steps of degradation are diverse because the two compounds differ from each other only in the nitro group (Figs. 6 and 7). Through the process, the composition of microorganisms changes dynamically.

The effect of the metal ions added to the oil shale and their amounts in the case of the two substrates confirm that not the same enzyme systems resulted in the degradation. Guzik et al.^[16] also reported cases when the concentration of the added metal ions greatly affected the enzymatic activities (sometimes the higher, sometimes the lower concentration was advantageous) and, consequently, the enzyme reaction rate as well.

Results of GC-MS measurements and the proposed degradation pathways of 4-nitrophenol and phenol

Sludge and supernatant samples were periodically taken from the reaction mixture during the degradation process, as well as after the complete elimination of the substrate indicated by HPLC-UV. After extraction and silylation, GC-MS measurement was conducted. There was not any difference between the results of the initial and middle parts, or between extraction from sludge and supernatant, considering the presence of identified intermediary degradation products.

In the case of 4-nitrophenol, the m/z signals of silylated products of hydroquinone (m/z : 239, 254, 112) and 4-nitrocatechol (m/z : 284, 299, 137) were detected as intermediates, along with those of 4-nitrophenol (m/z : 196, 211, 135) and other organic materials that originated from the oil shale in the sludge and supernatant samples. After 12 days, 4-nitrophenol was undetectable by HPLC-UV in the samples. Moreover, neither the substrate nor 4-nitrocatechol could be detected by GC-MS in the extracts of these samples. However, the quantity of hydroquinone was slightly above its detection limit. It is worth highlighting that the extracts of supernatants were up to approximately 150 times more concentrated than without extraction, considering their component concentrations. Based on the identified

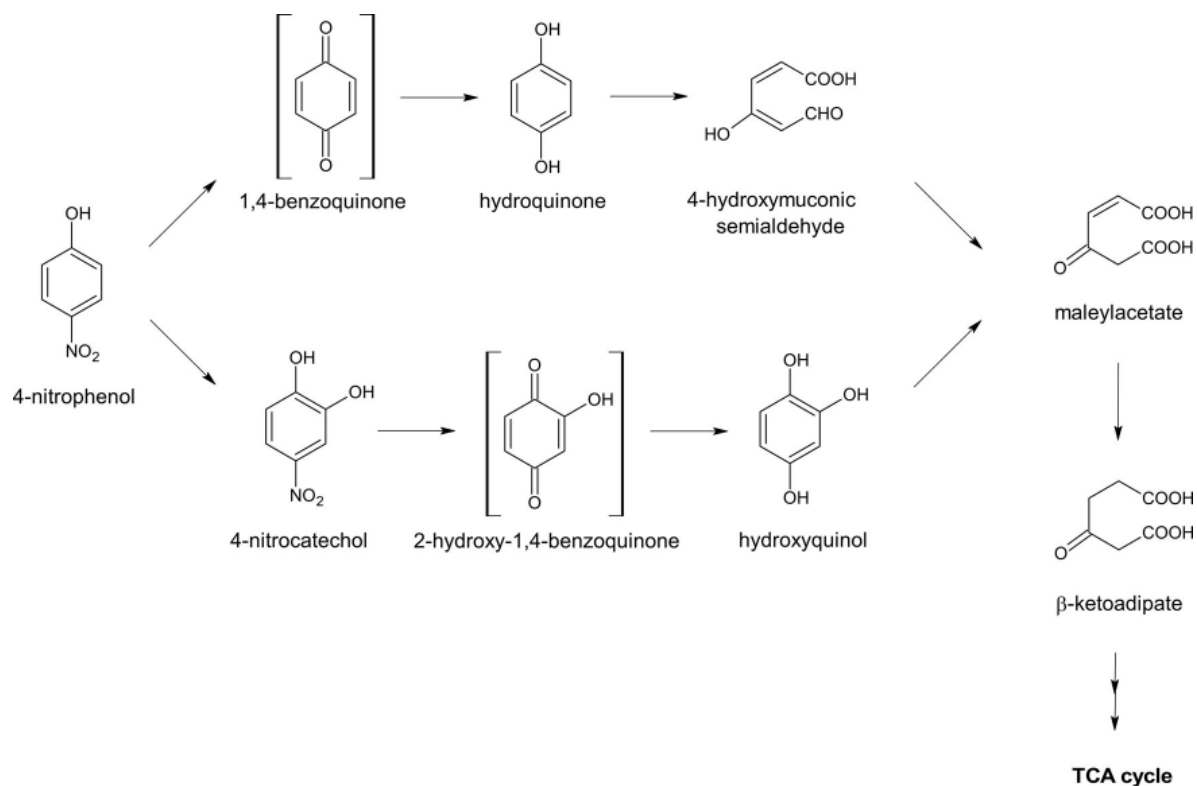


Figure 6. Proposed degradation pathway of 4-nitrophenol in the presence of oil shale.

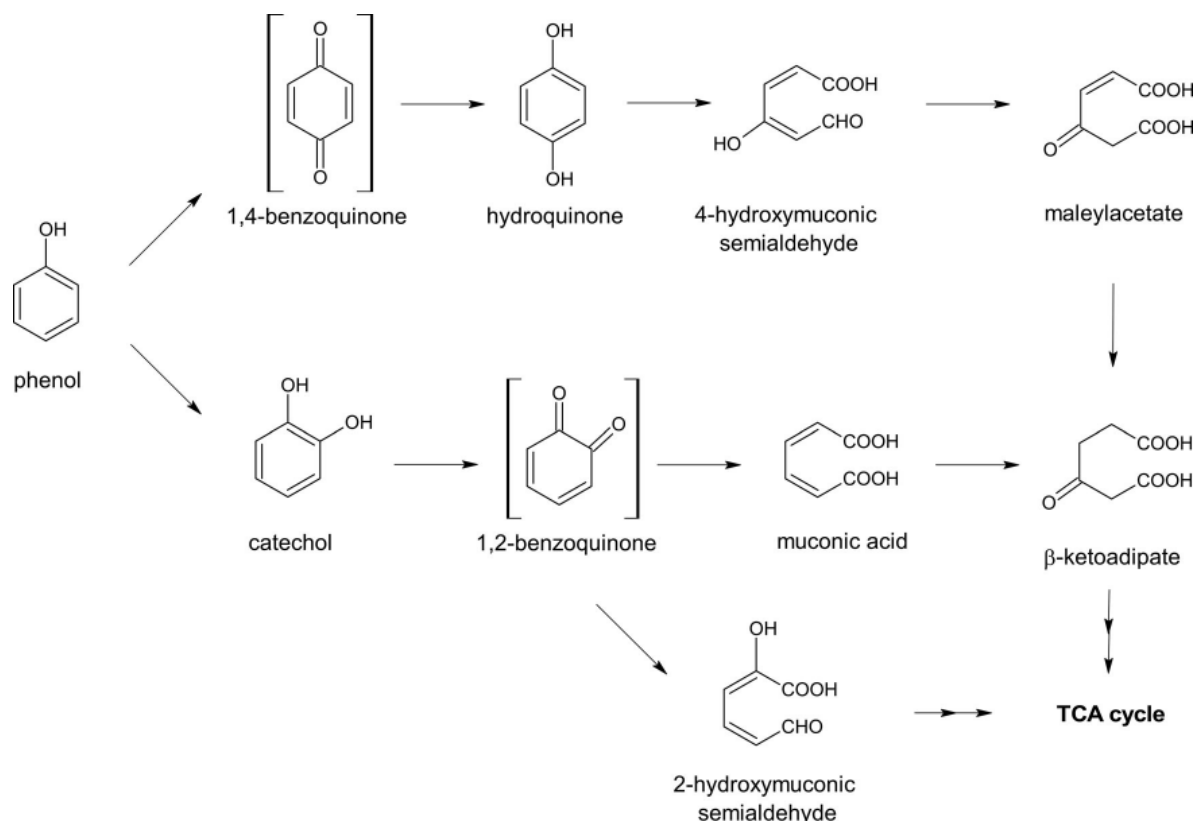


Figure 7. Proposed degradation pathway of phenol in the presence of oil shale.

intermediate compounds and the possible degradation routes published in the literature,^[3–5] the following pathway is suggested (Fig. 6). The possible decomposition route is bifurcated at the beginning as 4-nitrophenol could be transformed through hydroquinone and 4-nitrocatechol (or hydroxyquinol) pathways simultaneously.

Nitro group might be removed as nitrite ion, which could be further converted into nitrate ion (Fig. A2 in the Appendix). Presumably, microorganisms consumed nitrate as a nitrogen source. The compounds in the two pathways are converted into maleylacetate, which might be further transformed through β -ketoadipate and tricarboxylic acid

Table 1. Fitting parameters of the degradation curves described by the Hockey-stick model, and their DegT50 and DegT90 values.

Substrate	Swelling solution	k_1 (10^{-2} /day)	k_2 (1/day)	t_b (day)	R^2	DegT50 (day)	DegT90 (day)
4-Nitrophenol	Deionized water (reference base)	5.84	0.543	6.57	0.995	7.14	10.1
	154 mmol/L $MnCl_2$	5.76	0.730	5.77	0.991	6.26	8.47
	15 μ mol/L $MnCl_2$	3.49	1.099	7.53	0.995	7.92	9.39
Phenol	Deionized water (reference base)	8.87	0.898	5.41	0.983	5.65	7.44
	15 μ mol/L $FeSO_4$	11.5	0.856	3.74	0.986	4.05	5.93
	15 μ mol/L $MnCl_2$	10.7	2.707	3.91	1.000	4.01	4.61
	15 μ mol/L $ZnCl_2$	22.9	11.185	3.94	1.000	3.02	4.07

(TCA) cycle intermediates. Finally, these intermediates might enter the TCA cycle.

In the case of phenol, silylated products of hydroquinone (m/z : 239, 254, 112) and catechol (m/z : 254, 239, 151) as silylated intermediates, besides phenol (m/z : 151, 166, 77) and other organic materials released from oil shale were detected in the extracts which were taken during the degradation experiment. These components were detected already at the initial stage of the degradation process (after 1 day), and they were also present at the middle and the final stages of the process. Furuya et al.,^[29] van Schie and Young^[2] demonstrated that the degradation pathway of phenol in the presence of microorganisms proceeds through hydroquinone or catechol, respectively. In the presence of Maar-type oil shale containing a microbial community, similar reaction routes might take place, which is summarized in Figure 7. Analogically to the case of 4-nitrophenol, the route is bifurcated in the beginning. One degradation route is analogous to the hydroquinone pathway mentioned above, while another route might go through catechol, which is probably further degraded into both muconic acid and 2-hydroxymuconic semialdehyde, representing two alternative pathways. Muconic acid was further metabolized through β -keto adipate, which was a common intermediary degradation product of the hydroquinone pathway as well. Finally, 2-hydroxymuconic semialdehyde and β -keto adipate enter the TCA cycle via additional TCA intermediates.

In both cases (4-nitrophenol and phenol), the addition of iron(II), manganese(II), or zinc(II) ions to the oil shale did not modify the type of the detectable intermediates; thus, the proposed degradation pathways were not affected by these ions. Notably, the other intermediates, which are specified in Figures 6 and 7, could be present in the reaction mixture, but their quantity was lower than their detection limit. A similar observation was made by Rauch and Földényi,^[7] who investigated an other substrate, using similar oil shale, but not all of the intermediates derived from the proposed degradation pathway could be identified. Nonetheless, the detected intermediates were sufficient to depict the degradation routes.

Biodegradation kinetics of 4-nitrophenol and phenol

As mentioned above, degradation curves (concentration as a function of time) of 4-nitrophenol and phenol can be divided into two main sections: a slower initial (adaptation period), and a faster second decay phase. This kind of pattern can be well described by the Hockey-stick model (EU

FOCUS guidance).^[30] This model consists of two sequential curves. Both curves are expressed by first-order kinetics (Eqs. (1) and (2)). Although the model can handle the breakpoint, the single first-order kinetic model does not properly describe the second phase in each case. Nevertheless, combined usage of the first-order and zero-order kinetic model (Eqs. (1) and (3)) as a modified Hockey-stick model can be suitably applied to fit the data when the former model cannot suitably be utilized. This model can properly be applied when the oil shale was pretreated with sodium azide.

$$c(t) = c_0 \cdot e^{-k_1 \cdot t} \text{ for } t \leq t_b \quad (1)$$

$$c(t) = c_0 \cdot e^{-k_1 \cdot t_b} \cdot e^{-k_2 \cdot (t - t_b)} \text{ for } t > t_b \quad (2)$$

$$c(t) = c_0 \cdot e^{-k_1 \cdot t_b} - k_3 \cdot (t - t_b) \text{ for } t > t_b \quad (3)$$

where t is the time elapsed from the beginning of the degradation stage (day); t_b is the time of the breakpoint, when the rate constant or kinetic changes (day); $c(t)$ is the time-dependent concentration in the supernatant (μ mol/L); c_0 is the initial concentration of solute when the degradation stage started (when the adsorption equilibrium was reached) (μ mol/L); k_1 , k_2 are the rate constants of the first-order kinetic model (1/day); k_3 is the rate constant of the zero-order kinetic model (μ mol/(L·day)).

Accordingly, after the equations had been fitted to the data, and the parameters of the given curve had been determined, the times at which the initial concentration of substrate decreased by 50 and 90% (DegT50 and DegT90) were calculated. These values and parameters of the curves are listed in Tables 1 and 2.

As can be seen in Table 1, the values of k_1 are always smaller than those of k_2 because k_1 represents the rate constant of the adaptation period.

ANOVA ($\alpha = 0.05$) attested to the significant differences between the degradation curves of the reference bases and the cases of different treatments of oil shale ($p \leq 0.0008$ in every case).

When the oil shale was pretreated with sodium azide solution, k_1 values (Table 2) were smaller compared to their reference base (Table 1), the higher the concentration of sodium azide, the lower the k_1 rate constant can be obtained. Furthermore, the time of the breakpoint (t_b) appeared much later. Although k_3 is incomparable to k_2 , the prolonged second section of the degradation curves and the lower k_3 values at the higher concentrations of sodium azide indicate the slower degradation of substrates.

Table 2. Fitting parameters of the degradation curves described by the modified Hockey-stick model, and their DegT50 and DegT90 values.

Substrate	Swelling solution	k_1 (10^{-3} /day)	k_3 ($\mu\text{mol}/(\text{L day})$)	t_b (day)	R^2	DegT50 (day)	DegT90 (day)
4-Nitrophenol	5 g/L NaN_3	4.13	13.0	41.7	0.998	50.0	59.7
	10 g/L NaN_3	1.74	8.73	75.1	0.998	88.7	103.1
Phenol	5 g/L NaN_3	6.32	33.2	42.6	0.992	44.9	49.8
	10 g/L NaN_3	4.44	7.37	46.7	0.998	61.3	80.0

Effect of the initial concentration of substrate on its degradation

The initial concentration of 4-nitrophenol and phenol was increased (from 500 $\mu\text{mol}/\text{L}$) to 1000, 1500, and 2000 $\mu\text{mol}/\text{L}$ in order to investigate the changes in degradation time and kinetics. In every case, the degradation time was extended, but in different ways for the two compounds.

Having increased the initial concentration of 4-nitrophenol, it could be degraded slower. Its higher initial concentration induced a greater extent of elongation and a lower degradation rate. Hence, the t_b values increased, while the k_1 and k_2 rate constants decreased (Table 3). The required degradation time was 30, 49, and 125 days, respectively. In the case of the initial concentration of 2000 $\mu\text{mol}/\text{L}$, 4-nitrophenol was degraded proportionally much slower (Figure 8). This result might be related to the toxic effect of 4-nitrophenol (as a function of concentration) on the microbial community in the oil shale.^[6,31] In the slower phase, higher percentages of microorganisms were destroyed by the solution because of its toxicity, and the surviving ones could adapt to the environment more difficultly when the initial concentration was higher. In the faster second phase, the toxicity of 4-nitrophenol had an impact on the microorganisms, and this effect was dominant, especially at the highest investigated concentration range. In addition, the intermediates derived from 4-nitrophenol could also have an inhibitory effect on microorganisms^[32]; hence, higher initial concentrations of 4-nitrophenol could produce greater inhibitory effects in both the first and second phases. Chakraborty^[6] and Sam et al.^[31] investigated the concentration dependence of the degradation rate of 4-nitrophenol, and found that the rate displayed a maximum. Further increase of the concentration of 4-nitrophenol induced a decrease of the degradation rate. Thus, the results exposed in this work do not well agree with those in the reference, presumably because of the deviating investigated concentration ranges and microorganisms.

The degradation time for phenol was also increased when its initial concentration was enhanced, roughly proportionally in the concentration range investigated (Fig. 9). The required degradation time was 20, 28, and 45 days, respectively. The fitting parameters, DegT50 and DegT90 values, summarized in Table 3, show that the t_b values increased, k_1 and k_2 rate constants decreased with the increasing initial concentration of phenol. However, there are not uniform findings in the literature regarding the initial concentration dependence of the degradation rate of phenol. For example, Kwon and Yeom^[27] described that the degradation rate increased with increasing initial concentration of phenol, regarding the faster decay phase, while the slower (first) adaptation phase elongated. Oppositely, Sam et al.^[31] found

that the degradation rate decreases with increasing initial concentration. These seemingly contradictory results can be explained by the difference in microorganisms, in the extent and time of adaptation of microorganisms to the substrates, and the quantity of accumulated toxic intermediates during degradation.

The slope of the Michaelis-Menten curve, which corresponds to the rate constant, is higher in the lower concentration range and vice versa.^[33] Although supposedly not just one enzyme is responsible for the degradation of substrates, and considering the unusual degradation curve (including breakpoint), these results well agree with Michaelis-Menten kinetics if k_1 and k_2 rate constants are depicted separately as functions of the initial concentration of both substrates (Figs. A3 and A4 in the Appendix).

Reusability of oil shale as a degradation promoter material

After the degradation of the given substrate, the degradation effect of the same oil shale on the identical substrate was investigated. The used oil shale was washed overnight in a 0.01 mol/L CaCl_2 solution, and the supernatant was decanted. 250 mL of 4-nitrophenol or phenol solution (500 $\mu\text{mol}/\text{L}$ of 0.01 mol/L CaCl_2) was poured onto the washed oil shale. All the circumstances of the degradation process were identical to the above-described methods. The reusability of oil shale was studied in four cycles.

After the first and second re-usages of oil shale, the degradation time of substrates remarkably decreased, 4-nitrophenol and phenol were degraded faster compared to the first usage. Both substrates completely disappeared from the supernatants in 3.5 and 4.5 days. However, after the third and fourth re-usages of the oil shale, the degradation time increased to 5 and 7 days, respectively.

The first or previous usage(s) of oil shale can be regarded as a pre-adaptation step in which the microbial community in the oil shale adapted to the new environment containing the given substrate, as well as the accumulation of microorganisms whose enzyme systems were responsible for the degradation. Thus, these enzyme systems of the pre-adapted microorganisms could degrade 4-nitrophenol or phenol much faster. Additionally, the slower initial step disappeared because there was no need for another adaptation step. Nevertheless, these shortened degradation times of 4-nitrophenol and phenol were attenuated after the second re-usage, without reappearing in the slower initial step. Presumably, a part of the microbial community was lost during the washing and the consumable organic materials in the oil shale were reduced.

Table 3. Fitting parameters of the degradation curves and their DegT50 and DegT90 values when the initial concentration of substrates was increased.*

Substrate	Initial concentration of substrate (before adsorption) ($\mu\text{mol/L}$)	k_1 ($10^{-3}/\text{day}$)	k_2 ($10^{-2}/\text{day}$)	t_b (day)	R^2	DegT50 (day)	DegT90 (day)
p-Nitrophenol	500 (reference base)	58.4	54.3	6.57	0.995	7.14	10.1
	1000	24.9	25.3	12.9	0.995	14.4	20.7
	1500	11.9	22.8	33.8	0.993	35.1	42.2
	2000	5.63	7.46	89.2	0.989	91.7	113
Phenol	500 (reference base)	88.7	89.8	5.41	0.983	5.65	7.44
	1000	41.5	41.1	11.8	0.993	12.3	16.2
	1500	32.0	15.7	11.9	0.989	13.9	24.2
	2000	29.9	8.74	17.3	0.993	19.3	37.8

*The curves have been described by the Hockey-stick model (for comparison, the curve for the initial concentration of 500 $\mu\text{mol/L}$ (reference base) is also listed).

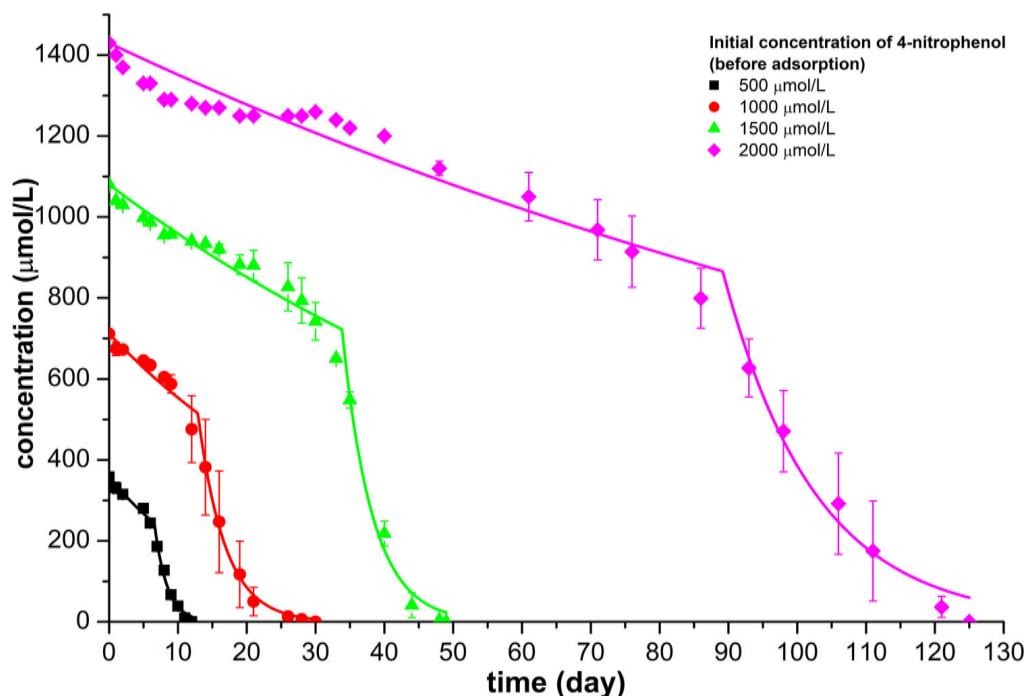


Figure 8. Degradation curves for various initial solute concentrations of 4-nitrophenol in the presence of oil shale. For comparison, the curve for the initial concentration of 500 $\mu\text{mol/L}$ (reference base) is also illustrated.

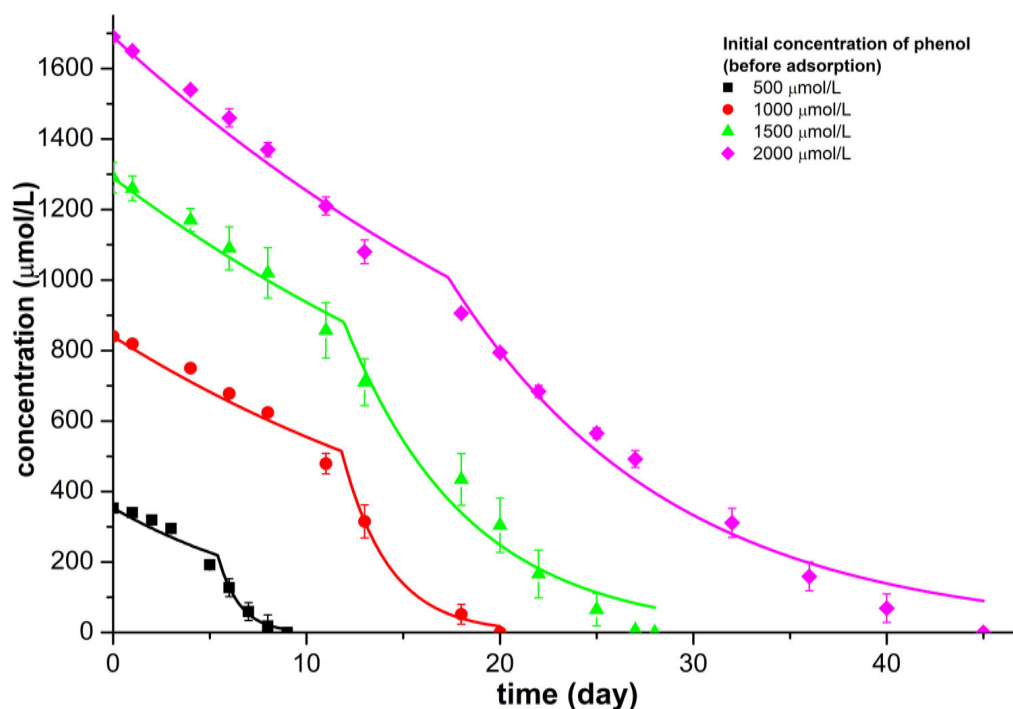


Figure 9. Degradation curves for various initial solute concentrations of phenol in the presence of oil shale. For comparison, the curve for the initial concentration of 500 $\mu\text{mol/L}$ (reference base) is also illustrated.

Practically, the reused oil shale could significantly shorten the degradation time of both substrates through two cycles. Hence, this is another way to increase the efficiency of oil shale in the degradation process. Furthermore, re-usage is generally not just a cost-efficient solution, but it can decrease the waste amount.

Results of the bioinformatics analysis

Figures A5–A7 (in the Appendix) depicts the relative abundance of bacteria at the genus level before and after the degradation of 4-nitrophenol or phenol.

Following the degradation of both substrates, the taxonomic distribution changed significantly. As can be seen from Figures A5–A7, most of the identified genera are soil bacteria belonging mainly to *Actinomycetales*. In the case of 4-nitrophenol, the relative abundance of *Actinomadura*, *Salinispora*, *Nocardioides*, and *Pseudonocardia* were highly decreased during the degradation, but the numbers of *Arthrobacter*, *Pedobacter*, and *Rhizobium* were increased, probably due to the selection pressure of the xenobiotic.

In the case of phenol, similarly to the previously described case, the relative quantities of *Actinomadura*, *Salinispora*, *Nocardioides*, and *Pseudonocardia* were lowered, and *Pedobacter*, *Bacillus* and *Altererythrobacter*, were increased. The taxonomy distributions at the genus level show that for the degradation of 4-nitrophenol and phenol, not the same microorganisms are responsible, considering their relative quantities. The alteration in the bacterial composition during biodegradation is frequent, other authors have also presented similar observations.^[34–36]

Conclusion

In this study, oil shale as a degradation promoter material was investigated by using two persistent aromatic compounds, 4-nitrophenol and phenol. In the presence of oil shale, these model pollutants were completely biodegraded in 12 and 9 days, respectively. Assuming that the biodegradation is catalyzed by metalloenzymes, four different cations, manganese(II), iron(II), copper(II), or zinc(II) ions were added to the oil shale, and the effect of the addition was studied on the degradation time. Manganese(II) ions could shorten the degradation time of 4-nitrophenol; iron(II), manganese(II), or zinc(II) ions could also reduce the decomposition period of phenol. Moreover, the reused oil shale could also biodegrade these model chemicals, even faster than the first-used oil shale for two cycles. GC-MS measurement revealed the proposed pathways of the biodegradation of the two chemicals. Intermediates of both compounds might end up in the TCA cycle. Microbiological studies revealed that bacteria were the primary source of biodegradation, and their relative abundance was investigated. These findings demonstrate that an extremely low-cost oil shale can be used not only as an adsorbent but also as a degradation promoter material. In the presence of oil shale, even persistent compounds can easily be biodegraded. In the

future, we will investigate how effectively oil shale can enhance the degradation of heterocyclic compounds.

Acknowledgment

The authors acknowledge the competent help of Dr. Gábor Csitári, Dr. Zsolt Valicsek, Dr. Erzsébet Szabó-Bárdos, Dr. Éva Makó, Miklós Jakab, Dr. Endre Domokos and Dr. Zoltán Bihari (Xenovaea Kft.).

Disclosure statement

The authors declare no conflict of interest.

Funding

This work was supported by the Széchenyi 2020 under the GINOP-2.2.1-15-2017-00037.

ORCID

Ottó Horváth  <http://orcid.org/0000-0002-5325-8430>

References

- [1] Awad, A. M.; Shaikh, S. M. R.; Jalab, R.; Gulied, M. H.; Nasser, M. S.; Benamor, A.; Adham, S. Adsorption of Organic Pollutants by Natural and Modified Clays: A Comprehensive Review. *Sep. Purif. Technol.* **2019**, *228*, 115719. DOI: [10.1016/j.seppur.2019.115719](https://doi.org/10.1016/j.seppur.2019.115719).
- [2] van Schie, P. M.; Young, L. Y. Biodegradation of Phenol: Mechanisms and Applications. *Bioremediat. J.* **2000**, *4*, 1–18. DOI: [10.1080/10588330008951128](https://doi.org/10.1080/10588330008951128).
- [3] Kimura, N.; Kitagawa, W.; Kamagata, Y. Biodegradation of Nitrophenol Compounds. In *Biological Remediation of Explosive Residues*, 1st ed.; Singh, S. N., Ed.; Springer: Switzerland, **2013**; pp 1–13. DOI: [10.1007/978-3-319-01083-0_1](https://doi.org/10.1007/978-3-319-01083-0_1).
- [4] Arora, P. K.; Srivastava, A.; Singh, V. P. Bacterial Degradation of Nitrophenols and Their Derivatives. *J. Hazard. Mater.* **2014**, *266*, 42–59. DOI: [10.1016/j.jhazmat.2013.12.011](https://doi.org/10.1016/j.jhazmat.2013.12.011).
- [5] Zhang, S.; Sun, W.; Xu, L.; Zheng, X.; Chu, X.; Tian, J.; Wu, N.; Fan, Y. Identification of the Para-Nitrophenol Catabolic Pathway, and Characterization of Three Enzymes Involved in the Hydroquinone Pathway, in *Pseudomonas* sp. 1-7. *BMC Microbiol.* **2012**, *12*, 27. DOI: [10.1186/1471-2180-12-27](https://doi.org/10.1186/1471-2180-12-27).
- [6] Chakraborty, B. Kinetic Study of Degradation of p-Nitro Phenol by a Mixed Bacterial Culture and Its Constituent Pure Strains. *Mater. Today Proc.* **2016**, *3*, 3505–3524. DOI: [10.1016/j.matpr.2016.10.034](https://doi.org/10.1016/j.matpr.2016.10.034).
- [7] Rauch, R.; Földényi, R. The Effect of Alginite on the Decomposition of the Herbicide propisochlor. *J. Environ. Sci. Health. B* **2012**, *47*, 670–676. DOI: [10.1080/03601234.2012.669212](https://doi.org/10.1080/03601234.2012.669212).
- [8] Zhu, Y.; Guo, J. Impact of Dichlorprop on Soil Microbial Community Structure and Diversity during Its Enantioselective Biodegradation in Agricultural Soils. *J. Environ. Sci. Health. B* **2020**, *55*, 974–982. DOI: [10.1080/03601234.2020.1802186](https://doi.org/10.1080/03601234.2020.1802186).
- [9] Solti, G. Alginit Tartalmú Műtrágyák, Földkeverékek és Talajjavító Anyagok. *AgrárUnió* **2003**, *4*, 33–34.
- [10] Hetényi, M. *Maar-Típusú Olajpalák Magyarországon*; JATE Press: Szeged, Hungary, **1996**.
- [11] Chen, X.; Murugananthan, M.; Zhang, Y. Degradation of p-Nitrophenol by Thermally Activated Persulfate in Soil System. *Chem. Eng. J.* **2016**, *283*, 1357–1365. DOI: [10.1016/j.cej.2015.08.107](https://doi.org/10.1016/j.cej.2015.08.107).
- [12] Weber, M.; Weber, M.; Kleine-Boymann, M. Phenol. In *Ullmann's Encyclopedia of Industrial Chemistry*, vol. 26.; Wiley-

- VCH: Germany, **2004**; pp 503–519. DOI: [10.1002/14356007.a19_299.pub2](https://doi.org/10.1002/14356007.a19_299.pub2)
- [13] Fang, H. H.; Liang, D. W.; Zhang, T.; Liu, Y. Anaerobic Treatment of Phenol in Wastewater under Thermophilic Condition. *Water Res.* **2006**, *40*, 427–434. DOI: [10.1016/j.watres.2005.11.025](https://doi.org/10.1016/j.watres.2005.11.025).
- [14] Abdu, N.; Abdullahi, A. A.; Abdulkadir, A. Heavy Metals and Soil Microbes. *Environ. Chem. Lett.* **2017**, *15*, 65–84. DOI: [10.1007/s10311-016-0587-x](https://doi.org/10.1007/s10311-016-0587-x).
- [15] Pereira, F. Manganese-Tolerant Bacteria from the Estuarine Environment and Their Importance in Bioremediation of Contaminated Estuarine Sites. In *Marine Pollution and Microbial Remediation*, 1st ed.; Naik, M. M.; Dubey, S. K., Eds.; Springer: Singapore, **2017**; pp 153–175.
- [16] Guzik, U.; Hupert-Kocurek, K.; Salek, K.; Wojcieszynska, D. Influence of Metal Ions on Bioremediation Activity of Protocatechuate 3,4-Dioxygenase from *Stenotrophomonas maltophilia* KB2. *World J. Microbiol. Biotechnol.* **2013**, *29*, 267–273. DOI: [10.1007/s11274-012-1178-z](https://doi.org/10.1007/s11274-012-1178-z).
- [17] Rajapaksha, R. M. C. P.; Tobor-Kaplon, M. A.; Bääth, E. Metal Toxicity Affects Fungal and Bacterial Activities in Soil Differently. *Appl. Environ. Microbiol.* **2004**, *70*, 2966–2973. DOI: [10.1128/AEM.70.5.2966-2973.2004](https://doi.org/10.1128/AEM.70.5.2966-2973.2004).
- [18] Molnár, M.; Földényi, R.; Horváth, O. Sorption of Potential Ionic Pollutants on Oil Shale and Its Non-Series Composite Sorbents. *Int. J. Environ. Sci. Technol.* **2021**, *18*, 3083–3098. DOI: [10.1007/s13762-020-03052-w](https://doi.org/10.1007/s13762-020-03052-w).
- [19] Tsuge, K.; Kataoka, M.; Seto, Y. Rapid Determination of Cyanide and Azide in Beverages by Microdiffusion Spectrophotometric Method. *J. Anal. Toxicol.* **2001**, *25*, 228–236. DOI: [10.1093/jat/25.4.228](https://doi.org/10.1093/jat/25.4.228).
- [20] Ghani, A.; Dexter, M.; Perrott, K. W. Extractable Carbon in Soils: A Sensitive Measurement for Determining Impacts of Fertilisation, Grazing and Cultivation. *Soil Biol. Biochem.* **2003**, *35*, 1231–1243. DOI: [10.1016/S0038-0717\(03\)00186-X](https://doi.org/10.1016/S0038-0717(03)00186-X).
- [21] Lázár, B.; Brenner, G. B.; Makkos, A.; Balogh, M.; László, S. B.; Al-Khrasani, M.; Hutka, B.; Bató, E.; Ostorházi, E.; Juhász, J.; et al. Lack of Small Intestinal Dysbiosis following Long-Term Selective Inhibition of Cyclooxygenase-2 by Rofecoxib in the Rat. *Cells* **2019**, *8*, 251. DOI: [10.3390/cells8030251](https://doi.org/10.3390/cells8030251).
- [22] Rauch, R.; Foldenyi, R. Investigation of Organic Matter Content of Hungarian Oil Shale and Its Influence on Sorption of 2,4-Dichlorophenol. *Period. Polytech. Chem. Eng.* **2020**, *64*, 230–237. DOI: [10.3311/PPch.15002](https://doi.org/10.3311/PPch.15002).
- [23] Kumar, M.; Monga, P.; Shukla, A.; Mehrotra, R. C. Botryococcus from the Early Eocene Lignite Mines of Western India: Inferences on Morphology, Taphonomy and Palaeoenvironment. *Palynology* **2017**, *41*, 462–471. DOI: [10.1080/01916122.2016.1259667](https://doi.org/10.1080/01916122.2016.1259667).
- [24] Kowalczyk, A.; Eyice, Ö.; Schäfer, H.; Price, O. R.; Finnegan, C. J.; van Egmond, R. A.; Shaw, L. J.; Barrett, G.; Bending, G. D. Characterization of Para-Nitrophenol-Degrading Bacterial Communities in River Water by Using Functional Markers and Stable Isotope Probing. *Appl. Environ. Microbiol.* **2015**, *81*, 6890–6900. DOI: [10.1128/AEM.01794-15](https://doi.org/10.1128/AEM.01794-15).
- [25] Shukla, S.; Naik, G.; Mishra, K. S. Potential Antimicrobial Activity of Bacterial Endophytes Isolated from *Flacourtia jangomas* (Lour.) Raeusch, a Less Explored Medicinal Plant. *J. Microbiol. Biotech. Food Sci.* **2015**, *4*, 473–477. DOI: [10.15414/jmbfs.2015.4.6.473-477](https://doi.org/10.15414/jmbfs.2015.4.6.473-477).
- [26] Fiori, A. K.; Gutuzzo, G.; de, O.; Sanzovo, A. W.; dos, S.; Andrade, D.; de, S.; Oliveira, A. L. M.; de Rodrigues, E. P. Effects of *Rhizobium tropici* Azide-Resistant Mutants on Growth, Nitrogen Nutrition and Nodulation of Common Bean (*Phaseolus vulgaris* L.). *Rhizosphere* **2021**, *18*, 100355. DOI: [10.1016/j.rhisph.2021.100355](https://doi.org/10.1016/j.rhisph.2021.100355).
- [27] Kwon, K. H.; Yeom, S. H. Optimal Microbial Adaptation Routes for the Rapid Degradation of High Concentration of Phenol. *Bioprocess Biosyst. Eng.* **2009**, *32*, 435–442. DOI: [10.1007/s00449-008-0263-z](https://doi.org/10.1007/s00449-008-0263-z).
- [28] Enguita, F. J.; Leitão, A. L. Hydroquinone: Environmental Pollution, Toxicity, and Microbial Answers. *Biomed. Res. Int.* **2013**, *2013*, 542168. DOI: [10.1155/2013/542168](https://doi.org/10.1155/2013/542168).
- [29] Furuya, T.; Hirose, S.; Osanai, H.; Semba, H.; Kino, K. Identification of the Monooxygenase Gene Clusters Responsible for the Regioselective Oxidation of Phenol to Hydroquinone in mycobacteria. *Appl. Environ. Microbiol.* **2011**, *77*, 1214–1220. DOI: [10.1128/AEM.02316-10](https://doi.org/10.1128/AEM.02316-10).
- [30] Panidepu, H.; Ram, S. K.; Cheernam, V.; Tyagi, R. D. Modeling Organic Pollutant Degradation Kinetics. In *Current Developments in Biotechnology and Bioengineering: Emerging Organic Micro-Pollutants*, 1st ed.; Varjani, S.; Pandey, A.; Tyagi, R. D.; Ngo, H. H.; Larroche, C., Eds.; Elsevier: Amsterdam, Netherlands, **2020**; pp 205–230. DOI: [10.1016/B978-0-12-819594-9.00009-7](https://doi.org/10.1016/B978-0-12-819594-9.00009-7).
- [31] Sam, S. P.; Tan, H. T.; Sudesh, K.; Adnan, R.; Ting, A. S. Y.; Ng, S. L. Phenol and p-Nitrophenol Biodegradations by Acclimated Activated Sludge: Influence of Operational Conditions on Biodegradation Kinetics and Responding Microbial Communities. *J. Environ. Chem. Eng.* **2021**, *9*, 105420. DOI: [10.1016/j.jece.2021.105420](https://doi.org/10.1016/j.jece.2021.105420).
- [32] Bhushan, B.; Chauhan, A.; Samanta, S. K.; Jain, R. K. Kinetics of Biodegradation of p-Nitrophenol by Different Bacteria. *Biochem. Biophys. Res. Commun.* **2000**, *274*, 626–630. DOI: [10.1006/bbrc.2000.3193](https://doi.org/10.1006/bbrc.2000.3193).
- [33] Svendsen, S. B.; El-Taliawy, H.; Carvalho, P. N.; Bester, K. Concentration Dependent Degradation of Pharmaceuticals in WWTP Effluent by Biofilm Reactors. *Water Res.* **2020**, *186*, 116389. DOI: [10.1016/j.watres.2020.116389](https://doi.org/10.1016/j.watres.2020.116389).
- [34] Gu, Q.; Wu, Q.; Zhang, J.; Guo, W.; Wu, H.; Sun, M. Community Analysis and Recovery of Phenol-Degrading Bacteria from Drinking Water Biofilters. *Front. Microbiol.* **2016**, *7*, 495. DOI: [10.3389/fmicb.2016.00495](https://doi.org/10.3389/fmicb.2016.00495).
- [35] Chen, R.; Ren, L.-F.; Shao, J.; He, Y.; Zhang, X. Changes in Degrading Ability, Populations and Metabolism of Microbes in Activated Sludge in the Treatment of Phenol Wastewater. *RSC Adv.* **2017**, *7*, 52841–52851. DOI: [10.1039/C7RA09225C](https://doi.org/10.1039/C7RA09225C).
- [36] Viggor, S.; Jøesaar, M.; Soares-Castro, P.; Ilmjärv, T.; Santos, P. M.; Kapley, A.; Kivisaar, M. Microbial Metabolic Potential of Phenol Degradation in Wastewater Treatment Plant of Crude Oil Refinery: analysis of Metagenomes and Characterization of Isolates. *Microorganisms* **2020**, *8*, 652. DOI: [10.3390/microorganisms8050652](https://doi.org/10.3390/microorganisms8050652).

Appendix

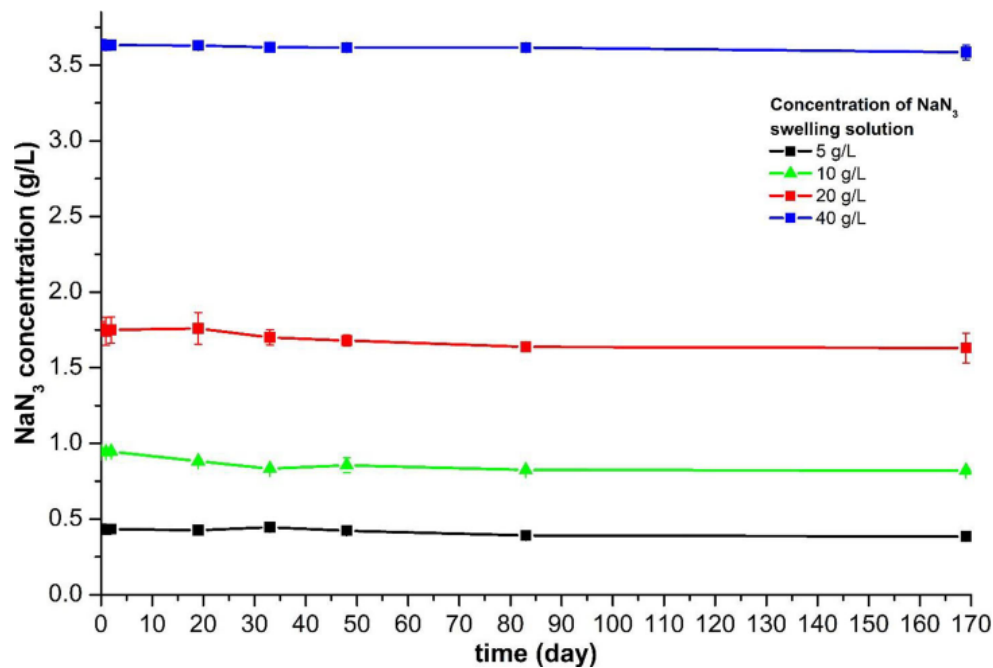


Figure A1. The concentration of sodium azide in the supernatant as a function of time.

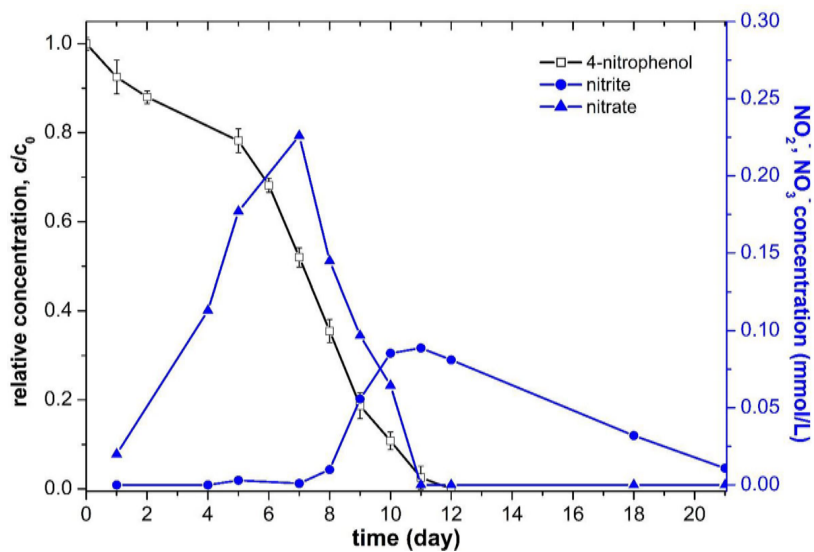


Figure A2. The concentration of nitrite and nitrate ions in the supernatant through the degradation of 4-nitrophenol.

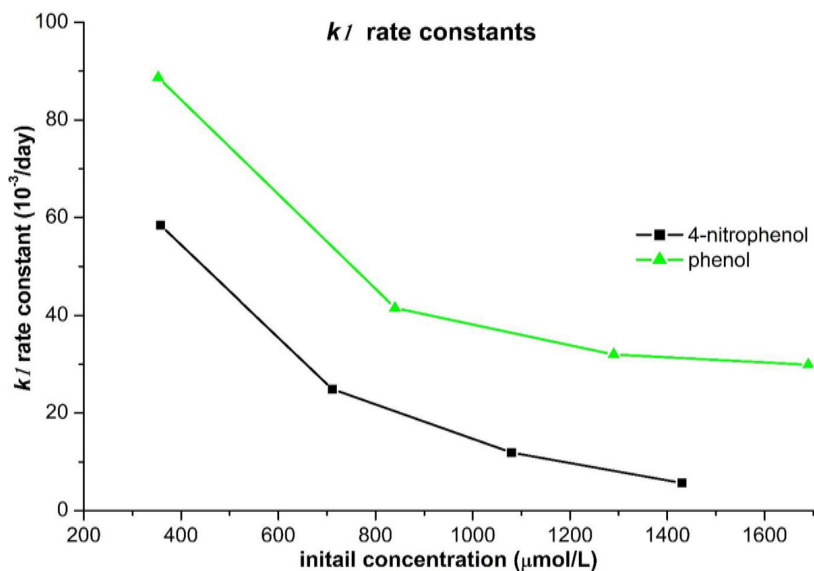


Figure A3. k_1 rate constants as a function of the initial concentration of substrate (the decrease of concentration during adsorption was taken into account when the initial concentrations were listed).

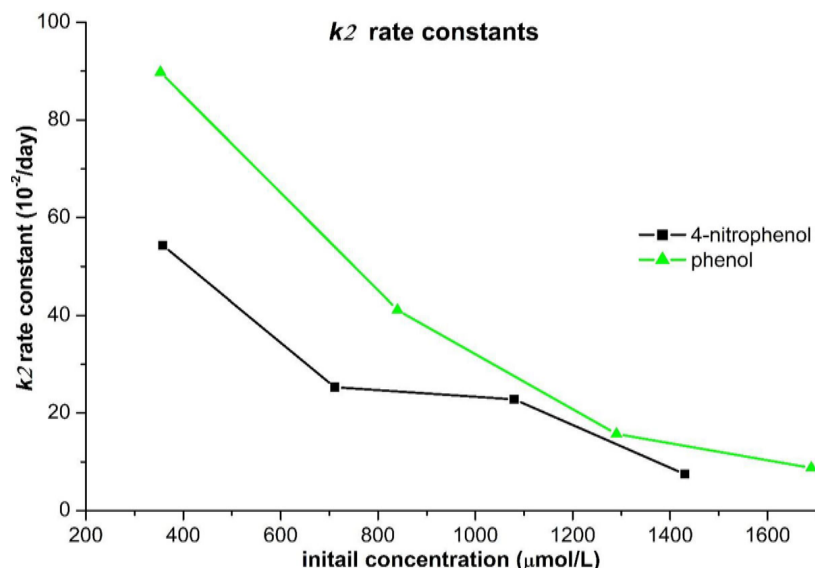


Figure A4. k2 rate constants as a function of the initial concentration of substrate (the decrease of concentration during adsorption was taken into account when the initial concentrations were listed).

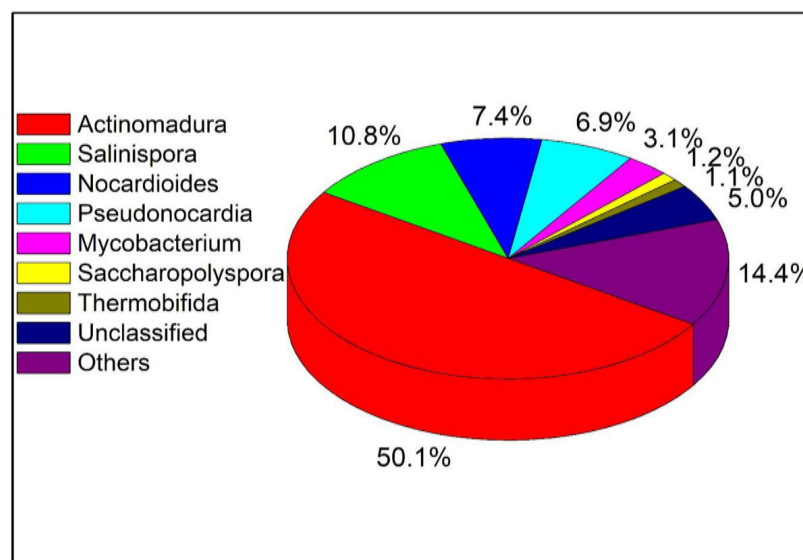


Figure A5. Relative abundance of bacteria in the oil shale before degradation experiments. The "Others" category represents the sum of all classifications beyond the top 8.

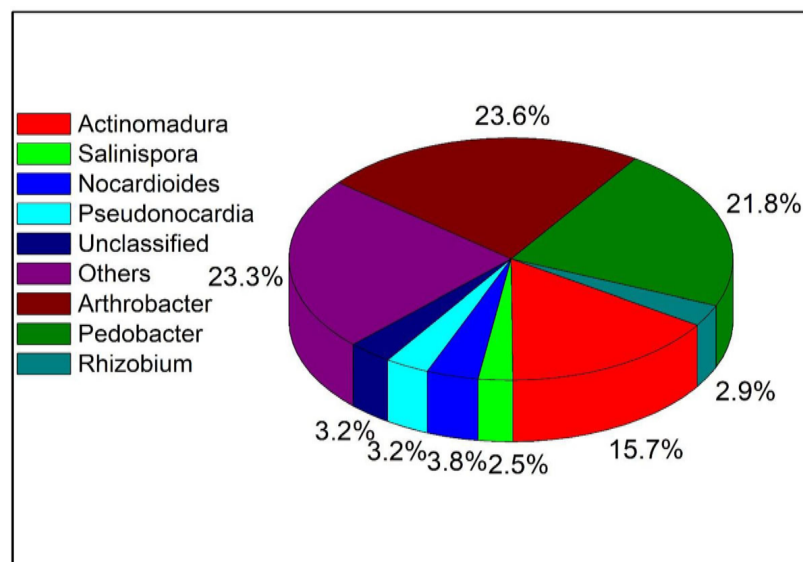


Figure A6. Relative abundance of bacteria in the oil shale after degradation of 4-nitrophenol. The "Others" category represents the sum of all classifications beyond the top 8.

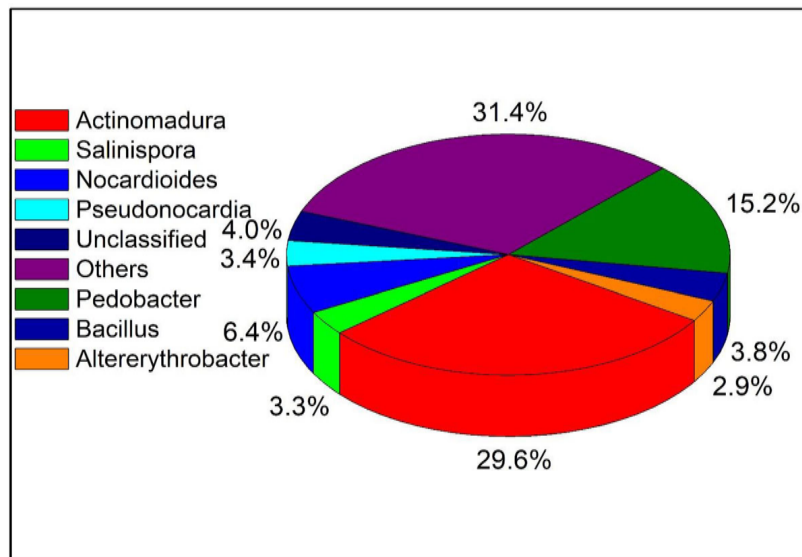


Figure A7. Relative abundance of bacteria in the oil shale after degradation of phenol. The “Others” category represents the sum of all classifications beyond the top 8.